Supplemental information

Adipocyte mesenchymal transition

contributes to mammary tumor progression

Qingzhang Zhu, Yi Zhu, Chelsea Hepler, Qianbin Zhang, Jiyoung Park, Christy Gliniak, Gervaise H. Henry, Clair Crewe, Dawei Bu, Zhuzhen Zhang, Shangang Zhao, Thomas Morley, Na Li, Dae-Seok Kim, Douglas Strand, Yingfeng Deng, Jacob J. Robino, Oleg Varlamov, Ruth Gordillo, Mikhail G. Kolonin, Christine M. Kusminski, Rana K. Gupta, and Philipp E. Scherer

Supplemental information

Adipocyte Mesenchymal Transition Contributes to Mammary Tumor Progression

Qingzhang Zhu, Yi Zhu, Chelsea Hepler, Qianbin Zhang, Jiyoung Park, Christy Gliniak, Gervaise H. Henry, Clair Crewe, Dawei Bu, Zhuzhen Zhang, Shangang Zhao, Thomas Morley, Na Li, Dae-Seok Kim, Douglas Strand, Yingfeng Deng, Jacob J Robino, Oleg Varlamov, Ruth Gordillo, Mikhail G. Kolonin, Christine M. Kusminski, Rana K. Gupta, and Philipp E. Scherer

Supplementary Figures

Figure S1. Adipocytes undergo de-differentiation during mammary tumor infiltration into the stroma
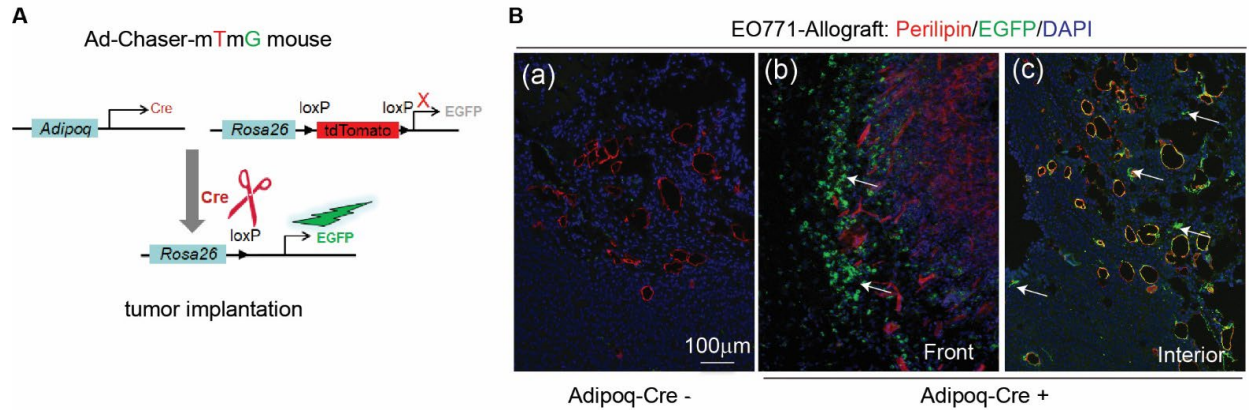

Figure. S1. Adipocytes undergo de-differentiation during mammary tumor infiltration into the stroma. Related to Figure 1. (A) Adipocyte lineage tracing scheme of dox-independent Ad-Chaser-mTmG mice used for tumor implantation. (B) Growth of ectopic tumor allograft results in mammary adipocyte de-differentiation in Ad-Chaser-mTmG mice (n=3). No EGFP$^+$ cells are present in tumors from Adipoq-Cre$^-$ mice (a). Arrows indicate de-differentiated EGFP$^+$/Perilipin$^-$ cells with fibroblast-like morphology in tumor invasive front (b) and in the core area (c). Scale bar, 100 μm.

Figure S2. Single-cell RNA-sequencing reveals adipocyte mesenchymal transition during mammary tumor progression
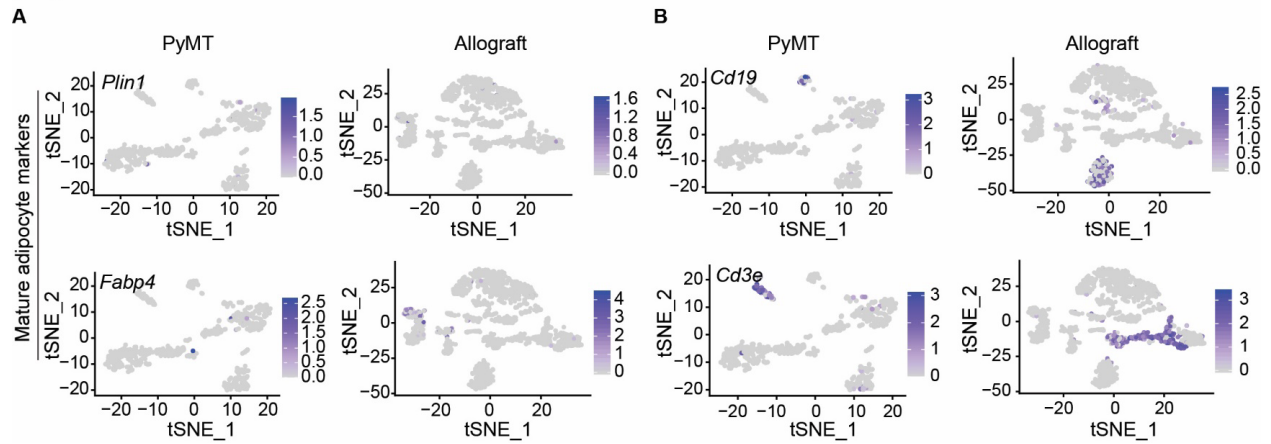

Figure. S2. Single cell-RNA sequencing reveals adipocyte mesenchymal transition during mammary tumor progression. Related to Figure 2. (A) None/few de-differentiated adipocytes express mature adipocyte markers. (B) Small populations of de-differentiated adipocytes are positive with specific cell markers of T cells and B cells.

Figure S3. Mammary tumor-induced de-differentiated adipocytes contribute to tumor microenvironment concerning inflammation and extracellular matrix remodeling
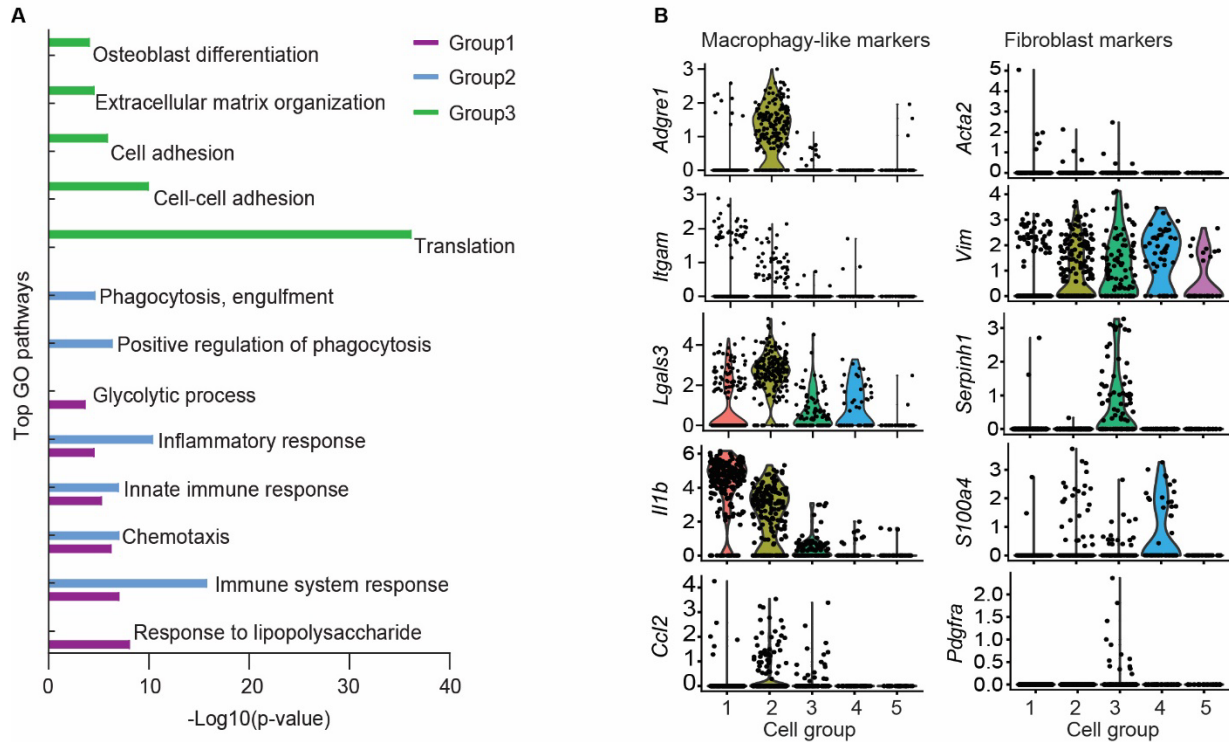

Figure. S3. Mammary tumor-induced de-differentiated adipocytes contribute to tumor microenvironment concerning inflammation and extracellular matrix remodeling. Related to Figure 3. (A) Gene ontology (GO) pathway enrichment analysis reveals de-differentiated adipocytes from AdipoChaser-PyMT tumor are likely involved in the processes of ECM remolding, and inflammatory and immune response. (B) Individual violin plots showing the expression levels and distribution of representative macrophage and fibroblast markers genes. The y axis is the log-scale normalized read count.

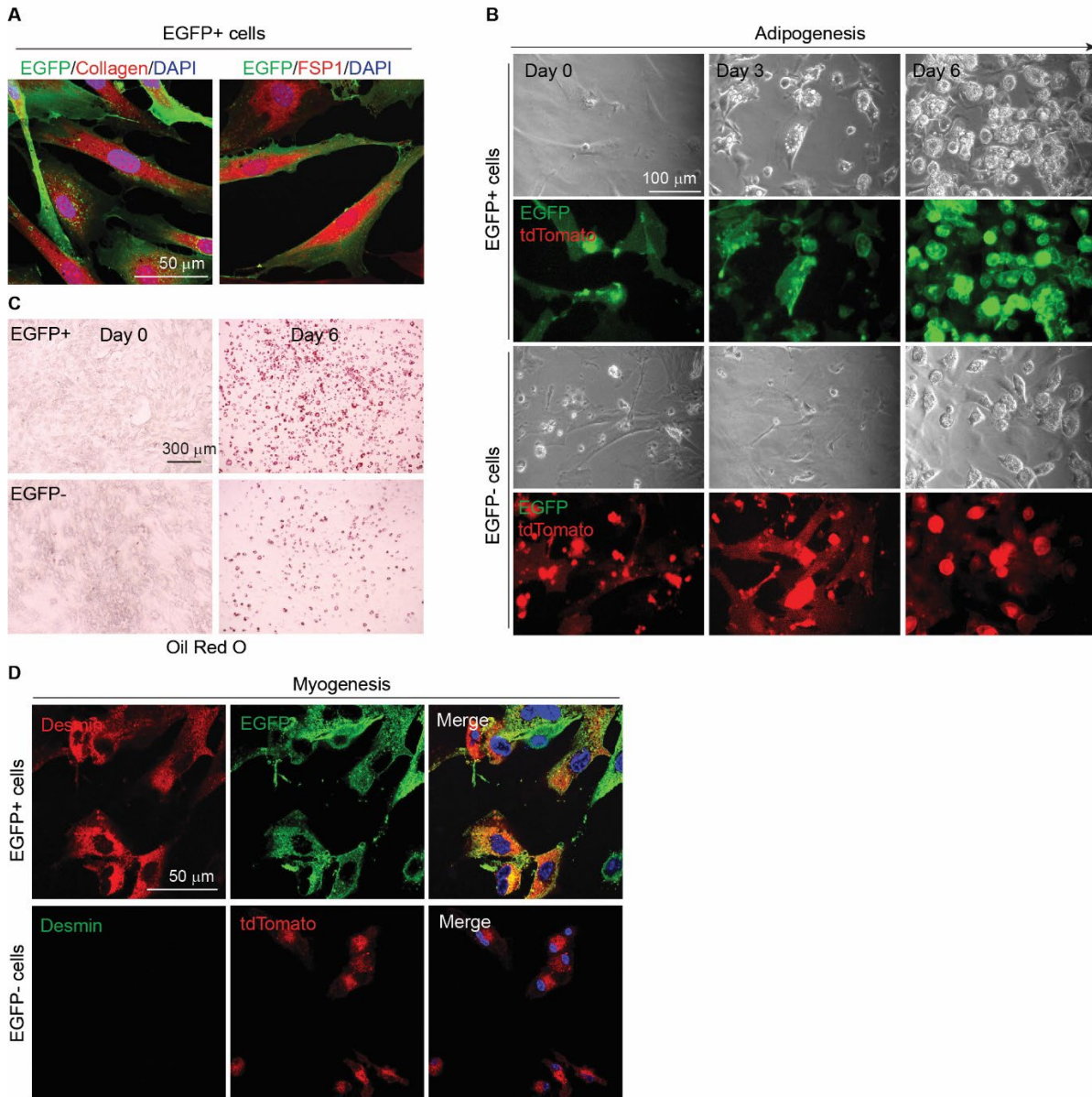**Figure S4. Tumor induced de-differentiated adipocytes display adipogenesis and myogenesis in vitro**

Figure. S4. Tumor induced de-differentiated adipocytes display adipogenesis and myogenesis in vitro. Related to Figure 3. (A) De-differentiated cells (EGFP$^+$, tdTomato$^-$) isolated from AdipoChaser-PyMT-tumor display fibroblast morphology and produce collagen and express fibroblast marker FSP1, Scale bar, 50 µm. (B) These EGFP$^+$ cells are more prone to re-differentiate to mature adipocytes (upper panel) as compared to tumor-associated fibroblasts (EGFP$^-$, tdTomato$^+$; lower panel). Scale bar, 100 µm. (C) Oil Red O staining at day 6 of adipogenic process. Scale bar, 300 µm. (D) Upon myogenic induction, these EGFP$^+$ cells are able to differentiate to Desmin$^+$ muscle-like cells, while EGFP$^-$ cells are not. Scale bar, 50 µm.

Table S1. Statistical analysis of histological images of each patient sample. Related to Figure 1 and Figure 3.
'Far' adipocytes (> 500 µm away from tumor lesion) and 'adjacent (adj)' adipocytes (within 500 µm surrounding tumor lesion) were analyzed.

Patient ID	Mean Adipocyte Area (µm²)	Adipocyte Count	Mean Thickness (µm)	Mean Highest observed Thickness (µm)	Mean Median Thickness (µm)	Fibrotic Fraction	Analytic Area (µm²)	Fibrotic Area (µm²)
13032-far	2898.4	561.0	16.4	43.6	11.8	0.3	1586777	471632.2
13049-far	2917.5	458.0	32.0	101.9	19.1	0.5	1586777	759989.7
13077-far	3805.7	172.0	12.0	31.3	8.7	0.2	1586777	335797.2
13152-far	2676.8	332.0	17.6	49.7	11.9	0.3	1586777	501546.7
13106-far	4561.5	313.0	22.5	71.4	13.7	0.3	1586777	471466.1
12867-far	3118.9	175.0	9.3	25.5	6.6	0.2	1586777	251260.3
12882-far	4412.6	126.0	20.5	61.8	13.0	0.3	1586777	477808.2
13109-far	4708.8	124.0	12.4	33.7	8.9	0.2	1586777	302115.5
12953-far	2681.0	336.0	19.7	55.1	13.2	0.4	1586777	558647.3
13032-adj	1029.2	934.0	34.5	111.6	21.4	0.7	1586777	1057292.4
13049-adj	1220.7	350.0	62.7	197.5	38.7	0.8	1586777	1182414.8
13077-adj	1368.6	343.0	81.8	256.1	49.7	0.7	1586777	1143331.8
13152-adj	1014.6	176.0	81.7	234.7	55.6	0.8	1586777	1193260.5
13106-adj	2258.1	230.0	108.0	316.0	72.9	0.6	1586777	945440.2
12867-adj	1860.5	410.0	63.5	190.6	42.5	0.7	1586777	1080189.8
12882-adj	1469.0	1156.0	28.1	90.3	17.3	0.5	1586777	793603.1
13109-adj	2223.8	25.0	47.3	143.4	30.6	0.7	1586777	1141760.8
12953-adj	1786.3	317.0	24.5	77.3	15.5	0.5	1586777	803390.4

Table S2. Characteristics of tumor samples from patients. Related to Figure 1.

Patient ID	Tumor subtype			Tumor site	Tumor form
13032	PR+	ER+	Her2-	Left	Invasive ductal carcinoma
13049	PR+	ER+	Her2-	Left	Invasive ductal carcinoma
13077	PR+	ER+	Her2-	Left	Invasive ductal carcinoma
13152	PR+	ER+	Her2-	Left	Invasive ductal carcinoma
13106	PR+	ER+	Her2-	Right	Invasive ductal carcinoma
12867	PR-	PR-	Her2-	Left	Invasive ductal carcinoma
12882	PR-	PR-	Her2-	Right	Invasive ductal carcinoma
13109	PR+	ER+	Her2+	Left	Invasive ductal carcinoma
12953	BRCA1 mutation			Right	Invasive ductal carcinoma

Table S3. Metabolic features of Ad-Xbp1s mice on chow-fed conditions. Related to Figure 5. Data presented as mean ± SEM, n=5 per genotype. Unpaired Student's t test was used for comparisons between genotypes. * $p < 0.05$; ** $p < 0.01$. NEFA, non-esterified fatty acids.

Parameters	WT		Ad-Xbp1s	
	Fed	**Fasted**	**Fed**	**Fasted**
Body weight (g)	26.1±0.9		23.3±0.7*	
Glucose (mg/dL)	164.9±3.8	83.2±4.1	186.0±6.5*	101.2±4.2*
Insulin (ng/ml)	0.9±0.2	0.4±0.1	0.8±0.1	0.5±0.1
NEFA (mM)	0.59±0.05	0.78±0.06	0.73±0.03*	0.89±0.06
Triglyceride (mg/dL)	82.9±11.9	61.1±5.6	83.5±11.9	45.1±3.4*
Cholesterol (mg/dL)	92.5±3.1	84.2±2.4	94.9±5.4	91.4±6.0
Adiponectin (μg/ml)	3.8±0.3	3.2±0.3	1.0±0.1**	0.8±0.1**
Leptin (ng/ml)	8.1±1.2	1.6±0.3	4.3±0.8*	1.5±0.5

Table S4. Quantitative PCR primer list. Related to STAR Methods.

Gene name	Protein name	Forward 5'-3'	Reverse 5'-3'
Adipoq	Adiponectin	TGTTCCTCTTAATCCTGCCCA	CCAACCTGCACAAGTTCCCTT
Lep	Leptin	GCGGTTGGATGGACTAGGAT	TTCGTCAGGGGCTTCCAAAG
Pparg 2	Peroxisome proliferator-activated receptor gamma, isoform 2	GCATGGTGCCTTCGCTGA	TGGCATCTCTGTGTCAACATG
Plin1	Perilipin 1	TACCTAGCTGCTTTCTCGGTG	GTGGGCTTCTTTGGTGCTGT
Col1a1	Collagen, type I, alpha 1	AGATGATGGGGAAGCTGGCAA	AAGCCTCGGTGTCCCTTCATT
Col3a1	Collagen, type III, alpha 1	CTGTAACATGGAAACTGGGGAAA	CCATAGCTGAACTGAAAACCACC
Col4a1	Collagen, type IV, alpha 1	CTGGCACAAAAGGGACGAG	ACGTGGCCGAGAATTTCACC
Col8a1	Collagen, type VIII, alpha 1	ACTCTGTCAGACTCATTCAGGC	CAAAGGCATGTGAGGGACTTG
Tgfb1	Transforming growth factor, beta 1	CTCCCGTGGCTTCTAGTGC	GCCTTAGTTTGGACAGGATCTG
Il6	Interleukin 6	CCGGAGAGGAGACTTCACAG	CAGAATTGCCATTGCACAAC
Il1b	Interleukin 1 beta	GCAACTGTTCCTGAACTCAACT	ATCTTTTGGGGTCCGTCAACT
Ccl2	Monocyte chemoattractant protein 1	AGCACCAGCCAACTCTCAC	TCTGGACCCATTCCTTCTTG
Cxcl2	C-X-C motif chemokine ligand 2	ACTAGCTACATCCCACCCACAC	GCACACTCCTTCCATGAAAGCC
Cxcl10	C-X-C motif chemokine ligand 10	CTCAGGCTCGTCAGTTCTAAGT	CCCTTGGGAAGATGGTGGTTAA
Cxcl14	C-X-C motif chemokine ligand 14	TGGACGGGTCCAAGTGTAAGT	TCCTCGCAGTGTGGGTACTTT
Rps16	40S ribosomal protein S16	GATTTGCTGGTGTGGATATT	TCTTTGATCTCCTTCTTGGA
Rps18	40S ribosomal protein S18	CTGGTTGATCCTGCCAGTAG	CGACCAAAGGAACCATAACT